

Chair of Optoelectronics
Institute of Computer Engineering
Universität Heidelberg

Annual Report 2014

CONTENTS

Staff	II
Foreword	III
Research Projects	IV
Publications in 2014	9
Imprint.....	10

STAFF



**Prof. Dr.
Karl-Heinz Brenner**
Head of Chair



Sabine Volk
Secretary



Wolfgang Stumpfs
Technical Assistant



Tim Stenau
PHD-Student



André Junker
PHD-Student



Max Auer
PHD-Student



Dr. Xiyuan Liu
PHD



Torsten Paul
Student



Armin Weyer
Student



FOREWORD

Dear reader,

This annual report describes the research activities of the chair of optoelectronics for the year 2014. The plenoptic camera is still in our research focus. While the emphasis last year was on wave-optical reconstruction, this year we have investigated a wave-optical refocusing. Another activity, running out this year was Mrs. Liu' work on phase retrieval. She finished her PhD. and therefore had to leave us. We are still investigating applications of diffractive overlapping lens arrays. Here we looked at the possibility of a Hartmann-Shack sensor with extremely long focal length. Finally we continued our work on localized fields as input to rigorous optical simulations.

We hope that many of the topics in this report will find your interest.

Karl-Heinz Brenner
Head of the chair

RESEARCH PROJECTS

A. Junker, T. Stenau and K.-H. Brenner <i>Digital Refocusing and Resolution Analysis of Wave-optically Reconstructed Plenoptic Camera Images</i>	1
X. Liu and K.-H. Brenner <i>Impact of Reduced Camera Resolution on Phase Retrieval</i>	2
A. Weyer and K.-H. Brenner <i>Shack-Hartmann Sensor with extended focal length using a diffractive optical element</i>	3
T. Stenau and K.-H. Brenner <i>Simulation of a Shack-Hartmann Sensor using diffractive lenses with overlapping aperture</i>	4
T. Paul and K.-H. Brenner <i>Investigation of refractive micro structures realized by photo-resist melting</i>	5
T. Stenau and K.-H. Brenner <i>Realisation of diffractive lenses with overlapping apertures and high numerical apertures</i>	6
K.-H. Brenner and M. Auer <i>Locality of Light Sources in Rigorous Optical Simulations</i>	7
M. Auer and K.-H. Brenner <i>Rigorous Light Propagation in Waveguides as one application of the Localized Input Field-RCWA (LIF-RCWA)</i>	8

Digital Refocusing and Resolution Analysis of Wave-optically Reconstructed Plenoptic Camera Images

A. Junker, T. Stenau and K.-H. Brenner

A light field camera, often also called plenoptic camera, measures not only the light intensity in a two-dimensional plane of interest, but records also directional information. This additional information can be used to manipulate images to a much larger extent after the image capture. A typical example of this kind is the refocusing operation, which uses the light field data to calculate a new intensity distribution in an arbitrary out of focus plane [1].

In the past image reconstruction algorithms were based on ray-tracing, which does not include diffraction at the aperture edges. Furthermore, present camera sensors have pixel sizes in the order of the wavelength of visible light, which means that the wave field is sampled to a degree where diffraction effects will play a role. Consequently, it can be assumed that algorithms based on ray-tracing are already at the limit of their validity. Therefore, we compare the resolution of our scalar wave-optical object reconstruction algorithm [2] to the results of a widely used ray-optical reconstruction procedure [1].

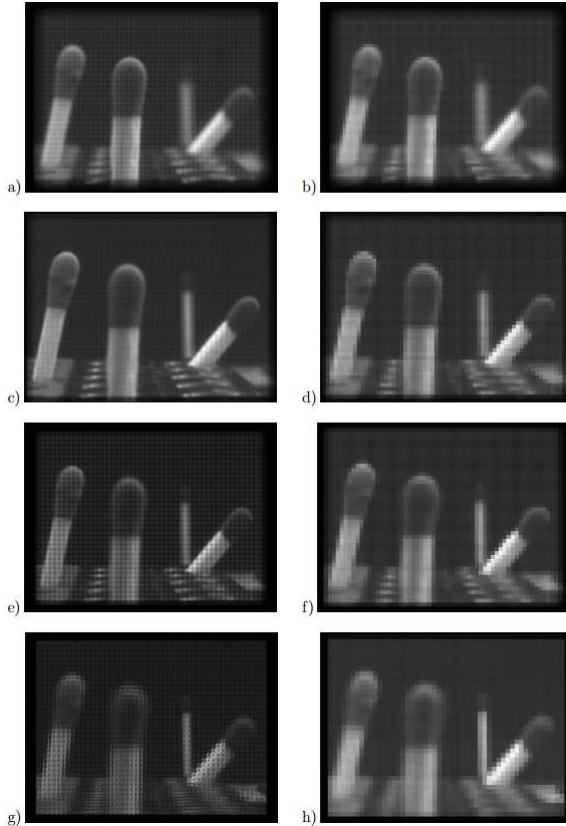


Fig. 1: Partly coherent wave-optical (left) and ray-optical (right) reconstruction of four matches into the planes a)/b) $g=8\text{cm}$, c)/d) $g=11\text{cm}$, e)/f) $g=13\text{cm}$, and g)/h) $g=30\text{cm}$. Main lens focused to infinity during light field capture.

Fig. 1 shows both wave-optical and ray-optical reconstructions of a light field of four matches positioned at different object distances g [3]. The refocusing ability is clearly demonstrated. A resolution enhancement of the wave-optical procedure compared to the ray-optical reconstruction is also visible. In order to confirm the increase in resolution, we determine the modulation transfer function (MTF) of the light field camera including the reconstruction procedure. For this purpose, we focus the main lens to infinity, place a pinhole of diameter $d=10\mu\text{m}$ at different object distances g and carry out a reconstruction from the light field data. The magnitude of the Fourier transform of this response corresponds to the MTF. From the width σ_v of the MTF, it is possible to estimate the spatial resolution according to $\sigma_x = (2\pi\sigma_v)^{-1}$.

Fig. 2 shows the effective feature size for both the wave-optical and ray-optical reconstruction procedure [3]. We find that the effective resolution in the wave-optical reconstruction lies by an almost constant factor of two above the resolution of the ray-optical reconstruction. For small g the spot size of the wave-optical reconstruction appears to approach the ray-optical binning diameter. Note, however, that for $g < 14\text{cm}$ the image of the pinhole becomes significantly larger than one detector pixel, thus we cannot regard the pinhole as a point source anymore.

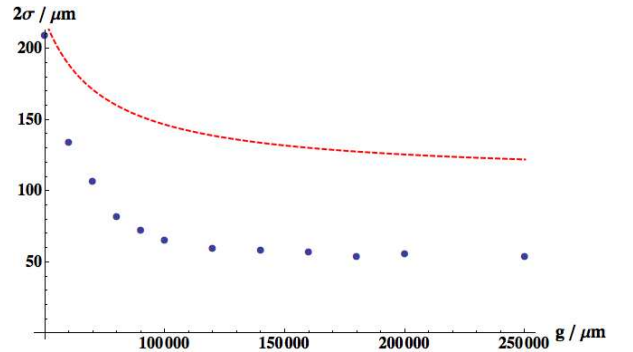


Fig. 2: Blue spots: effective feature size $2\sigma_x$ of the reconstructed image as a function of the main lens object distance g . Red dashed: feature size of the ray-optical reconstruction compensated for the expansion of the field of view [2].

References:

- [1] R. Ng, "Digital Light Field Photography" – PhD Thesis, Stanford University, (2006)
- [2] A. Junker, T. Stenau, K.-H. Brenner, "Scalar Wave-optical Reconstruction of Plenoptic Camera Images", Appl. Opt., Vol. 53, No. 25, 5784-5790, (2014)
- [3] A. Junker, "Wave-optical Reconstruction of Plenoptic Camera Images", Master Thesis, Universität Heidelberg, (2013)

Impact of Reduced Camera Resolution on Phase Retrieval

X. Liu and K.-H. Brenner

Considered as an imaging technique, phase retrieval may be used for the recovery of complex light distributions, without the need for any imaging lenses. This raises the question, if the resolution limitation for phase retrieval is still determined by the Abbe-formula.

Phase retrieval is an iterative method using multi-plane intensities of a defocused object wave. The central element is the camera, recording the multi-plane intensities. Here we investigate the impact of a reduced camera resolution on the reconstruction quality using numerical simulations. For this purpose we apply two different non-paraxial propagation methods: the angular spectrum propagation (AS) in near field and the Engelberg-Ruschin approximation (ERA) [1] in the far field.

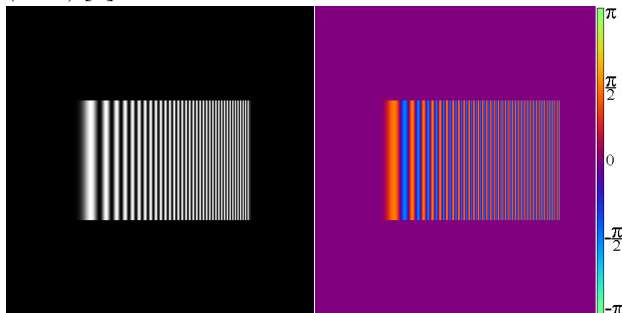


Fig. 1: Original test amplitudes, left: pure amplitude object; right: pure phase object (color palette)

In numerical simulations, we can retrieve the amplitude and the phase of a complex object separately. Figure 1 shows the original data: the amplitude of an amplitude object and the phase of a pure phase object.

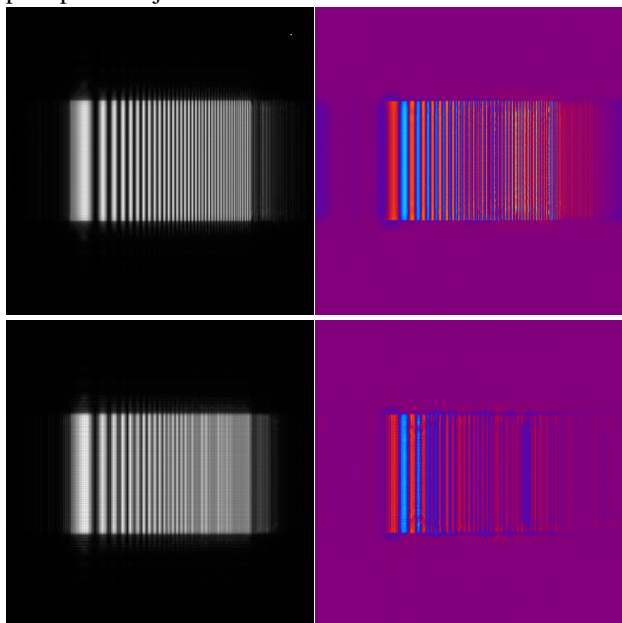


Fig. 2: Reconstruction in the near field (AS): amplitudes (left) and phase (right) with camera resolution reduced by a factor of 2 (top) and 4 (bottom).

Figures 2 and 3 present the corresponding reconstructions in the near field (fig. 2) and the far field (fig. 3).

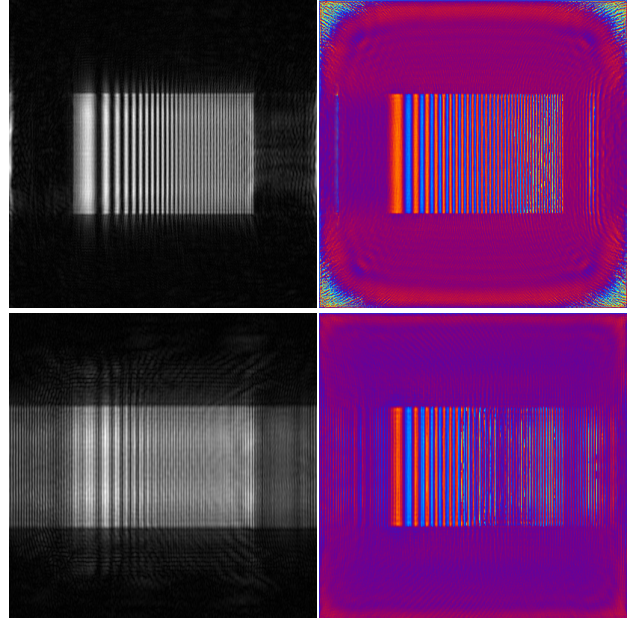


Fig. 3: Reconstructions in far field (ERA): amplitudes (left) and phase (right) with camera resolution reduced by a factor of 2 (top) and 4 (bottom)

For near field propagation, one can clearly observe a low-pass characteristic for amplitude objects and a band-pass characteristic for phase objects; for far field propagation, the observation is exactly the opposite. i.e. a band-pass characteristic for amplitude objects and a low-pass characteristic for phase objects. A comparison of reconstruction quality in the near and far field reveals that: for amplitude objects the reconstruction in the near field (AS) is better than in the far field (ERA); for phase objects, however, the reconstructions in the far field (ERA) is better than in the near field (AS).

In conclusion, a reduced camera resolution does have an effect on the reconstruction quality of phase retrieval. All relevant observations are summarized in table 1.

Reconstruction in	Amplitude object	Phase object
Near field (AS)	TP / +	BP / -
Far field (HNFF)	BP / -	TP / +

Table 1: Comparison of reconstructions; TP/+: low-pass characteristic and good quality; BP/-: band-pass characteristic and bad quality

Reference:

- [1] Y. M. Engelberg, S. Ruschin, "Fast method for physical optics propagation of high-numerical aperture beams", *JOSA A*, Vol. **21**, No. 11, 2135-2145, (2004)

Shack-Hartmann Sensor with extended focal length using a diffractive optical element

A. Weyer and K.-H. Brenner

The Shack-Hartmann (SH) sensor is one of the most common tools for wavefront sensing with applications in meteorology as well as closed loop wavefront correction in astronomy. The angular sensitivity of the SH-sensor is basically determined by the two parameters: focal length and spot size. The spot size also determines the focal intensity, which in case of limited number of photons also determines the quality of localization and thus the sensitivity. Therefore, a SH sensor with long focal length and small spot size should be ideal for high angular sensitivity.

With refractive lenses, there is a fixed relationship between lens diameter, focal length and spot size. Thus long focal length and small spot size can be only achieved at the expense of reduced sampling distance. With overlapping diffractive lenses, this fixed relationship can be overcome by adjusting the overlap between the lenses. A design for such a lens array is shown in fig. 1.

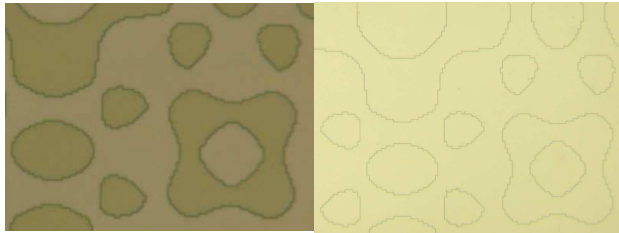


Fig. 1: Binary phase of the DOE, left: original resist, right: twofold copy: resist - PDMS- UV-curable polymer.

The picture demonstrates that the structures can be copied first into PDMS and in a second step into UV-curable polymer. The parameters of this design are: focal length: 12 cm, lens period: 563.2 μm , NA: 0.06 and spot size: 40 μm . A measurement of the spot array is depicted in fig. 2.

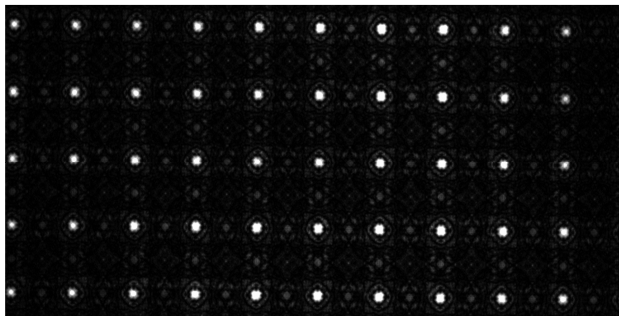


Fig. 2: Spot array intensity recorded at a distance of 120 mm from the DOE

From calculation, we can conclude, that a detectable shift of 2 μm is obtained, when the incident wavefront is tilted by 3.5 arcsec.

In order to verify this theoretical result, the optical set-up in fig. 3 was used. The collimating lens was mounted on a stage to be able to shift it by a given amount. The resulting radius of the spherical wave is

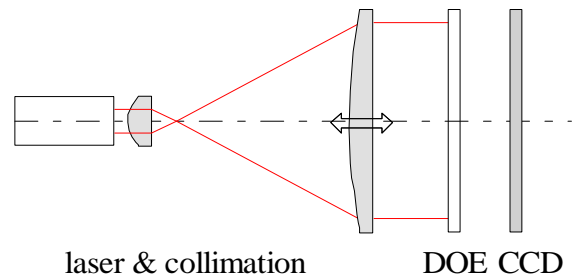


Fig. 3: Measurement set-up to test the diffractive SH-sensor. Parameters of the collimating lens. $f=160$ mm, $D=30$ mm.

given by (f : lens focal length, z : distance focal point - lens)

$$R_w = \frac{f \cdot z}{f - z} \quad (1)$$

At $z = f$ the light is collimated. A shift $z = f - \epsilon$ results in a wavefront radius of R_w and the tilt angle at the lens edge is given by $\vartheta = \text{atan}(R_L / R_w)$.

Consequently, a shift of 28 μm should result in a wavefront tilt of 3.4 arcsec at the lens edge. These theoretical results could be confirmed with a precision of 3%. This demonstrates, that a SH-sensor with diffractive optical lenses is indeed possible. With more elaborate spot position techniques, the spot center can be determined down to 0.5 μm and the minimum slope angle, that is detectable is 1 arcsec.

Reference:

- [1] R. Shack, B. C. Platt, "History and Principles of Shack-Hartmann wavefront sensing", Journal of Refractive Surgery, Vol. 17, No. 5, 573-577, (2001)

Simulation of a Shack-Hartmann Sensor using diffractive lenses with overlapping aperture

T. Stenau and K.-H. Brenner

The Shack-Hartmann sensor is an optical instrument designed to measure wavefronts. It is used to detect the aberrations of an optical system. Typical applications are characterization of optical components and measurement of aberrations in astronomy and ophthalmology.

The main component of a Shack-Hartmann sensor is a micro lens array placed in front of a camera so that a non aberrated wave produces foci in the camera plane. These foci are located centred behind each micro lens. For an aberrated wave, the local tilt of the incoming wave is translated in a lateral shift of the focal spot on the camera. The aberrated wavefront can be approximated from these local tilts.

We investigated the use of diffractive lenses with overlapping aperture instead of a refractive lens array by scalar simulation. For lenses with overlapping aperture, the overlap factor determines the ratio between the effective aperture size and the lens pitch.

The use of lenses with overlapping apertures promises dense sampling of the incoming wave and long focal length at the same time [1]. Therefore, we choose to simulate a micro lens array with 12 cm focal length and 495 μm pitch between the focal spots. With these specifications, local tilts of $\sim 2 \mu\text{rad}$ should be measurable assuming a localization accuracy of 1/10 of a 2.2 μm sized camera pixel.

The angular spectrum propagation and thin element approximation was used for light propagation. The centroiding is based on thresholding and linear weighting. Fig. 1 shows an example for the spot localisation in the image plane.

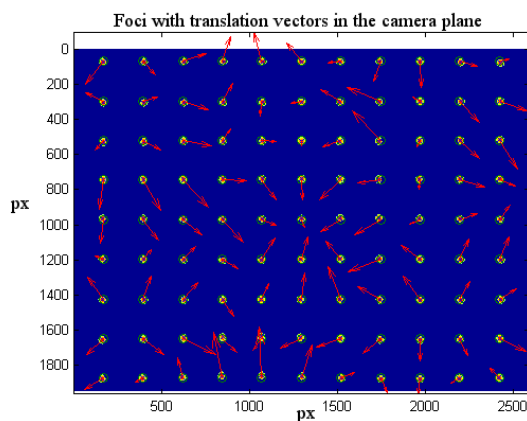


Fig. 1: Localisation of the foci in the sensor plane after thresholding. The red vectors show the shifts of the spots against the undisturbed position (scaled).

The reconstruction of the actual wave front defined by the local gradients was implemented using shifted radial basis functions. [2]

Different diffractive micro lens arrays with overlapping factors between 2 and 6 were simulated and compared with a refractive micro lens array and ground truth data.

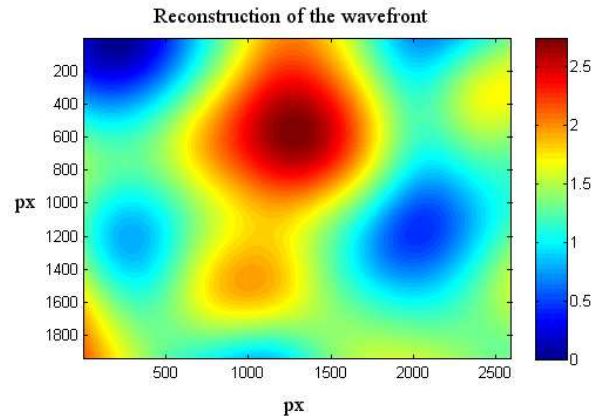


Fig. 2: Reconstruction of a random wave front obtained from a Shack-Hartmann sensor with a diffractive micro lens and overlap factor of 3.

Fig. 2 shows an example for a reconstruction of a random wave front. The simulated diffractive micro lens array has an overlap factor of 3.

We demonstrated that wave front reconstructions are possible with diffractive lens arrays with overlapping aperture. Comparing the results with the ground truth data indicates that the requirements on smoothness of the wave aberrations are more stringent than for refractive micro lens arrays. The reason for this is the overlap of the lenses. The smoother the original phase, the more accurate is the reconstruction with diffractive lenses with overlapping aperture.

References:

- [1] X. Liu, T. Stenau, K.-H. Brenner “Diffractive micro lens arrays with overlapping apertures”, 11th Euro-American Workshop on Information Optics (WIO) in Quebec, CA, (2012)
- [2] U. Maier, J. Hoffmann, K.-H. Brenner, “Surface Reconstruction from gradient data”, Jahrestagung der Deutschen Gesellschaft für angewandte Optik e. V. (DGaO) in Esslingen, (2008)

Investigation of refractive micro structures realized by photo-resist melting

T. Paul and K.-H. Brenner

Photoresist melting is an important method for the fabrication of refractive micro-lenses [1]. The surface shape is a result of the interaction of adhesion and surface tension and is mostly determined by the shape of the base area. If we choose a circular base area, the resulting elements are well known spherical micro lenses. For other shapes of the base area, more general refractive phase elements are possible. One example is a rectangular base shape, resulting in cylindrical micro lenses.

For the fabrication, we use the standard photoresist AZ9260, because of its thermal properties and because the layer thickness can be adjusted in a wide range. The illumination masks are written by laser lithography, available at the chair. The first step in the fabrication is spin coating a suitable layer thickness onto a glass substrate. Subsequently the exposure takes place in a mask aligner. After development, a thermal reflow process is applied. Finally, we replicate the structures in a double replication process. First we produce a negative of the structure in PDMS. Second, we fill the PDMS structure with UV-hardenable acrylate, thus producing a positive copy with homogeneous refractive index.

For the design of the base area, we apply a minimization algorithm, which minimizes the surface area while keeping the volume constant. The area is given by

$$\begin{aligned} A &= \iint \sqrt{1 + (\partial_x h)^2 + (\partial_y h)^2} dx dy \\ &= \iint \int_0^{2\pi} d\varphi \int_0^R r \sqrt{1 + (\partial_r h)^2} dr \end{aligned} \quad (1)$$

and the volume by

$$V = \iint h(x, y) dA = const \quad (2)$$

For the minimization we use an Euler-Lagrange type differential equation:

$$\frac{d}{dr} \frac{\partial}{\partial (\partial_r h)} L - \frac{\partial}{\partial h} L = 0 \quad (3)$$

with the Lagrangian:

$$L = \lambda r \sqrt{1 + (\partial_r h)^2} - hr \quad (4)$$

The result of this minimization algorithm agrees very well with the experimental results.



Fig. 1: Cylindrical micro lenses, left: in resist, middle: in PDMS, right: in UV-hardenable acrylate.

Figure 1 demonstrates that the original resist structure (left) can be copied reliably into PDMS (middle) and in a second step into UV-curable polymer (right).

The second part of the optimization procedure concerns the light propagation through these surface structures. For this, we used the WPM-method [2]. It can be considered as an extension of the BPM for unrestricted numeric apertures. In the example in fig. 2, we were interested in the maximum acceptance angle of such a dome-shaped lens.

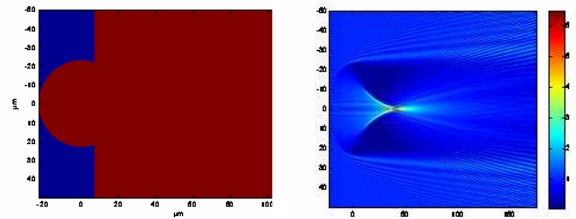


Fig. 2: Light propagation through a dome-shaped micro lens index distribution (left) using the WPM-method.

Applications of generalized refractive micro lenses can be found e.g. in light field imaging [3], where spatial and directional information is recorded.

References:

- [1] D. Daly, R. F. Stevens, M. C. Hutley, N. Davies, "The manufacture of microlenses by melting photoresist", Measurement Science and Technology, Bd. 1, BRISTOL: IOP PUBLISHING LTD, 759-766, (1990)
- [2] K.-H. Brenner, W. Singer, "Light propagation through microlenses: a new simulation method", Appl. Opt., Vol. 32, No. 26, 4984 - 4988, (1993)
- [3] A. Junker, Tim Stenau, K.-H. Brenner, "Wave optical reconstruction of plenoptic camera images", 7th International Workshop on Advanced Optical Imaging & Metrology (Fringe), 117-122, DOI: 10.1007/978-3-642-36359-7_14, ed. W. Osten, 08.-11.09.2013, Nürtingen, (2013)

Realisation of diffractive lenses with overlapping apertures and high numerical apertures

T. Stenau and K.-H. Brenner

The parallel scanning microscope aims to fill the gap between the high resolution point scanning methods and the low resolution and large field of view microscopes. [1] One of the key components of the parallel scanning microscope is a micro lens array which illuminates the specimen in a spot wise manner.

Due to the nature of diffractive optics, lens arrays with overlapping aperture can be designed, thus a dense illumination grid of localized foci is possible. For manufacturing purposes the DOE-phase is binarized.

Incorporating the fact that biological specimens are mostly protected by a cover slip, the cover slips influence on a high NA focus can be corrected already in the design process by accounting for the propagation inside the cover slip glass.

In cooperation with the Karlsruhe Micro-Nano-Facility, two diffractive elements for a parallel scanning microscope were fabricated. Figure 1 shows one period of the binary phase for two different lens arrays with overlapping aperture.

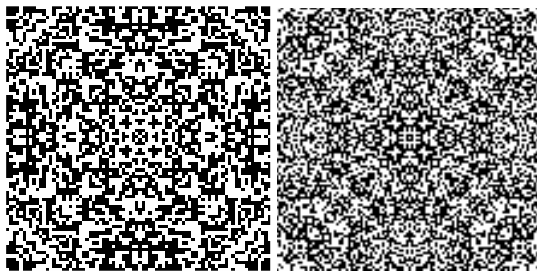


Fig. 1: Design periods of a moderate and high numerical aperture lens with overlapping aperture

Both periods are $44 \mu\text{m}$ and the focal length is 2 mm . The feature size of the left element is $0.55 \mu\text{m}$, whereas the feature size of the right element is $0.40 \mu\text{m}$. This enables numerical apertures of 0.48 and 0.75 at the wavelength of 532 nm . The overall size of each lens array is $13.2 \text{ mm} \times 13.2 \text{ mm}$, it contains 300×300 repetitions of the period.

The structure was written into resist with e-beam lithography and was transferred to the chromium layer by wet etching. Afterwards, the surface was treated with reactive ion etching and the residual chromium was removed. Images of one period of the fabricated elements are shown in Figure 2.

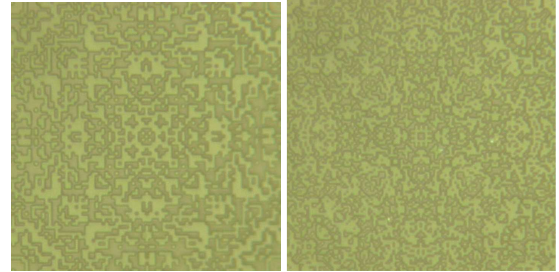


Fig. 2: Periods of the fabricated moderate and high numerical aperture lens array

These lens arrays are used in the high parallel scanning microscope. Scalar simulations of the intensity profiles, including a passage through a $150 \mu\text{m}$ cover slip are shown in Figure 3 for both elements.

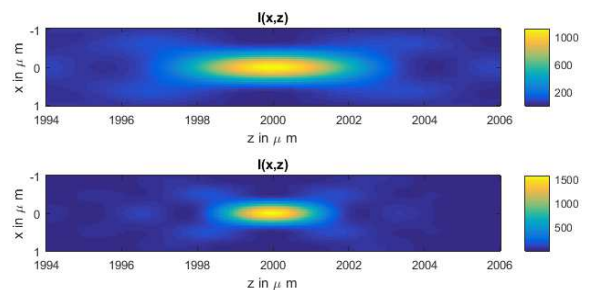


Fig. 3: Scalar simulation of the intensity profile after passing through a $150 \mu\text{m}$ cover slip. The top image the profile in the xz -plane for the numerical aperture of 0.48 , the bottom profile is for the numerical aperture of 0.75 .

The scalar simulation matches the well known equations for the focal shape. The lateral diameter is proportional to the inverse numerical aperture, whereas the axial diameter is proportional to the inverse numerical aperture squared.

Reference:

[1] K.-H. Brenner, T. Stenau, M. Azizian, “Entwicklung eines scannenden Mikroskops mit diffraktiven Mikrolinsen”, Jahrestagung der Deutschen Gesellschaft für angewandte Optik e. V. (DGaO) in Braunschweig, (2013)

Locality of Light Sources in Rigorous Optical Simulations

K.-H. Brenner and M. Auer

Modal simulation methods typically assume an infinitely extended plane wave as the input illumination. In many practical application scenarios, like in microscopy with structured illumination or in projection lithography, the locality of the illumination plays an important role. The usual approach is to decompose the input field distribution into a superposition of plane waves with different k-vectors and different polarization modes (TE, TM). By transition from a TE-TM-decomposition to a purely cartesian description, the problem can be treated with matrix methods, making the additional application of rotation matrices and a final summation obsolete [1].

In a cartesian description, assuming homogeneous layers, the field components can be written as two-component vectors. According to Maxwell theory, they are related by

$$\mathbf{H}_\perp = \mathbf{C} \cdot \mathbf{E}_\perp \quad (1)$$

where the perpendicular index indicates that only x- and y-components are used and \mathbf{C} is a 2x2 matrix containing the local refractive index and the weighted direction vector. The sign of the matrix depends on whether we consider forward- or backward propagating waves. The electric field in the layer is a superposition

$$\mathbf{E}_{\perp,j} = (\mathbf{T}_{\perp,j} \exp(ik_0 \tau_z z) + \mathbf{R}_{\perp,j} \exp(-ik_0 \tau_z z)) \exp(ik_0 \tau_\perp r_\perp - i\omega t). \quad (2)$$

The last phase term is identical in all layers. Thus the first term is sufficient for a description. We can represent \mathbf{E} and \mathbf{H} in a uniform layer in vectorial form as

$$\begin{pmatrix} \mathbf{E}_{\perp,j} \\ \mathbf{H}_{\perp,j} \end{pmatrix} = \mathbf{Q}(\boldsymbol{\tau}) \cdot \mathbf{P}(\boldsymbol{\tau}, z) \cdot \begin{pmatrix} \mathbf{T}_{\perp,j} \\ \mathbf{R}_{\perp,j} \end{pmatrix} \quad (3)$$

The continuity at the interfaces leads to a relation between adjacent layers:

$$\mathbf{S}_{j+1} = \mathbf{Q}_{j+1}^{-1} \cdot \mathbf{Q}_j \cdot \mathbf{P}_j \cdot \mathbf{S}_j, \quad (4)$$

where \mathbf{S} is the stacked forward (T) and backward (R) propagation vector. Considering $2M+1$ modes, all quantities are now vectors of length $4(2M+1)$. A problem with N layers can be represented as

$$\begin{pmatrix} \mathbf{T}_{N+1} \\ \mathbf{0} \end{pmatrix} = \mathbf{S}_{N+1} = \mathbf{M} \cdot \mathbf{S}_0 = \mathbf{M} \cdot \begin{pmatrix} \mathbf{T}_0 \\ \mathbf{R}_0 \end{pmatrix} \quad (5)$$

with the product matrix

$$\mathbf{M} = \mathbf{M}_N \cdot \mathbf{M}_0, \quad \mathbf{M}_j = \mathbf{Q}_{j+1}^{-1} \cdot \mathbf{Q}_j \cdot \mathbf{P}_j. \quad (6)$$

\mathbf{T}_0 describes the inhomogeneous illumination mode distribution in the incident region and \mathbf{T}_{N+1} , \mathbf{R}_0 are

the quantities to solve for. For improved stability, an ETMA-approach like in [2] can be used. Fig. 1 considers the case of no layer and $n_0 = n_{N+1} = 1$. All the modes within an NA of 0.5 have a strength of 1. The input polarization is linear (left) and radial (right):

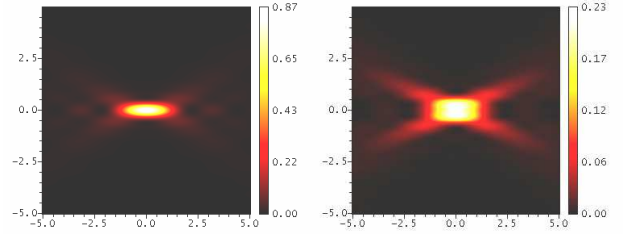


Fig. 1: Multimode treatment of a focus with NA 0.5. left: linear polarization; right: radial polarization.

In fig. 2 a typical problem of lithographic imaging is shown. The complex amplitude of the illumination follows from Fourier transformation of the illumination pattern, which here is a tribar pattern with 95 nm bar width. The polarization is linear and the layers are (water, resist, quartz). The depth of exposure in this configuration would not expose the resist fully.

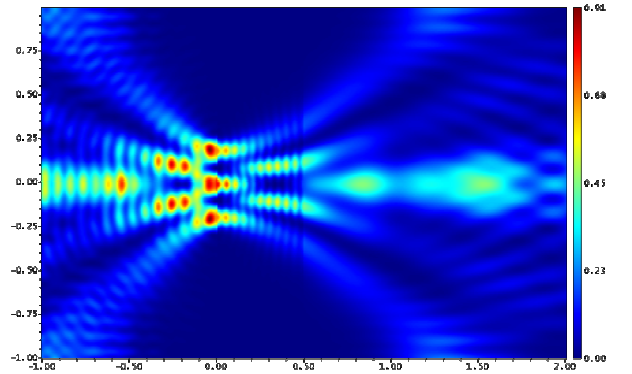


Fig. 2: High-NA-lithographic imaging of a tribar structure with 95 nm bar width using linear polarization and a wavelength of 193 nm. Axes are in units of μm .

References:

- [1] Moharam, M. G. et al., "Formulation for stable and efficient implementation of the rigorous coupled-wave analysis of binary gratings", *JOSA A*, Vol. **12**, No. 5, 1068-1076, (1995)
- [2] Moharam, M. G. et al., "Stable implementation of the rigorous coupled-wave analysis for surface-relief gratings: enhanced transmittance matrix approach", *JOSA A*, Vol. **12**, No. 5, 1077-1086, (1995)
- [3] Auer, M., Brenner, K.-H., "Localized input fields in the rigorous coupled-wave analysis", *JOSA A*, Vol. **31**, No 11, 2385-2393, (2014)

Rigorous Light Propagation in Waveguides as one application of the Localized Input Field-RCWA (LIF-RCWA)

M. Auer and K.-H. Brenner

With the LIF-RCWA[1] we developed an efficient extension to the Rigorous Coupled Wave Analysis (RCWA) that allows localized analysis of diffraction problems. Typical examples include localized input fields such as Gaussian beams interacting with a diffractive structure.

The analytical solution of light propagation in optical waveguides is only possible for a small number of simple geometries. A numerical alternative for arbitrary waveguides is offered by the LIF-RCWA, which in addition is able to describe waveguide coupling as well as leakage losses.

In order to demonstrate the performance of the method, a simple dielectric planar waveguide is used for reference: The refractive index of core and cladding are 1.47 and 1.46 respectively and the waist of the incident Gaussian beam is $\sigma = 3.5 \mu\text{m}$ at a wavelength of $\lambda = 1.55 \mu\text{m}$.

The analytical model[2] for the fundamental modes in a planar waveguide with core thickness of $d = 12 \mu\text{m}$ predicts three distinct propagative TE-modes for the incident angles $\pm\theta_1 = 2.024 \text{ deg}$, $\pm\theta_2 = 4.006 \text{ deg}$ and $\pm\theta_3 = 5.852 \text{ deg}$ as illustrated in Fig. 1.

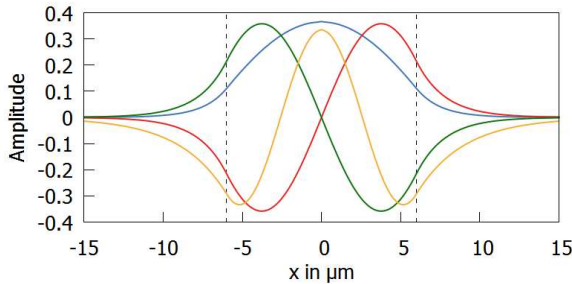


Fig. 1: Analytical waveguide modes (1th in blue, 2th in green and red, 3th in yellow)

Propagating these modes with their corresponding amplitudes through the waveguide analytically results in a distinct pattern that can be observed in Fig. 2a.

The numerical model for the LIF-RCWA includes an environment, in which the incident light beam is focused onto the entrance of the waveguide and in which the light leaves the waveguide at the end. In order to avoid additional interference by internal reflections at both ends of the waveguide, the refractive index of the surrounding is set to 1.47 – equal to the waveguide’s core. Since the diffraction problem is periodic in lateral direction in the RCWA, the period is chosen sufficiently large ($P = 125 \mu\text{m}$) with a weak absorbing boundary at the edges of the period in order to suppress crosstalk between the different periods.

Fig. 2b shows the result of the numerical calculation using the LIF-RCWA. The emerging pattern inside the

waveguide matches the analytical solution of Fig. 2a.

Furthermore, fig. 2b shows the coupling into the waveguide and the leakage due to a mismatch between the Gaussian incident beam and the propagative waveguide modes.

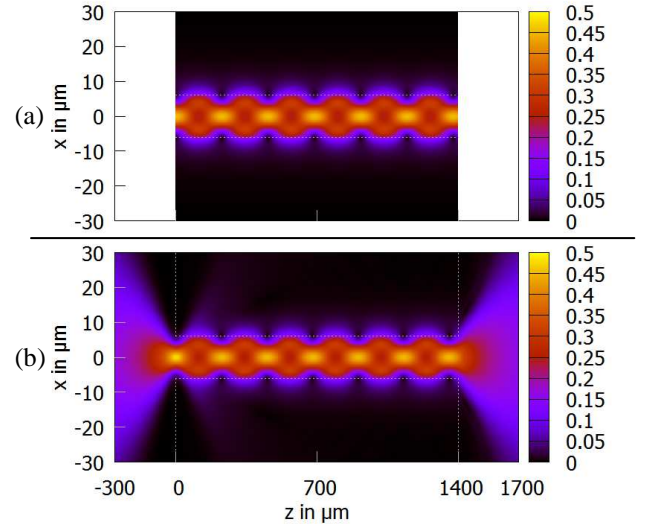


Fig. 2: Electric field distribution $|E|$ in a waveguide from (a) analytical model, (b) LIF-RCWA simulation (245 modes)

The mode matching between the Gaussian beam and the analytical waveguide modes can be determined by an overlap integral. Because all leakage should be absorbed by the boundaries in the numerical calculation, the analytically derived overlap integral should be equal to the transmission efficiency in the RCWA. In fact, Fig. 3 shows perfect agreement of the two for an increasing beam waist in a single-mode setup with $d = 3.72 \mu\text{m}$.

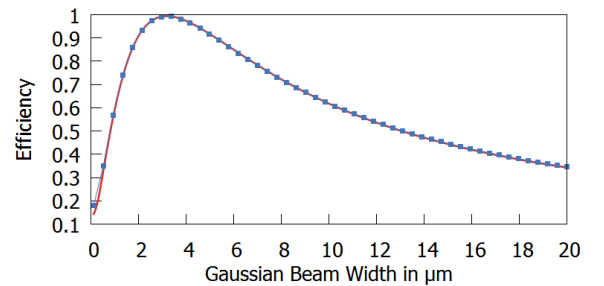


Fig. 3: Comparison between analytically derived mode matching degree (solid red) and numerically calculated transmission efficiency (dotted blue)

References:




- [1] M. Auer, K.-H. Brenner, “Localized input fields in rigorous coupled-wave analysis” – JOSA A., Vol. **31**, No. 11, 2385-2393, (2014)
- [2] B. E. A. Saleh and M. C. Teich, “Planar dielectric waveguides”, Fundamentals of Optics (Wiley), 299 –305, (2007)

PUBLICATIONS

1. X. Liu, K.-H. Brenner, "Phase Retrieval with a Diffractive Micro Lens Array", International Journal of Optomechatronics, Taylor & Francis, Vol. **8**, Issue 4, 251-259, ISSN: 1559-9612 print / 1559-9620 online, DOI:10.1080/15599612.2014.942926, (2014)
2. A. Junker, T. Stenau, K.-H. Brenner, "Scalar wave-optical reconstruction of plenoptic camera images", Applied Optics **53**, No. 25, 5784 – 5790, (2014)
3. M. Auer, K.-H. Brenner, "Localized input fields in rigorous coupled-wave analysis", J. Opt. Soc. Am. A, **31**, No. 11, 2385 – 2393, (2014)
4. T. Paul, K.-H. Brenner, "Untersuchung und Anwendung von Schmelzackstrukturen in der Mikrooptik", (Online-Zeitschrift der Deutschen Gesellschaft für angewandte Optik e. V.), ISSN: 1614-8436-urn:nbn:de:0287-2014-P034-8, 115. Jahrestagung, 10.-14. Juni 2014, Karlsruhe, (2014)
5. K.-H. Brenner, M. Auer, "Lokalität von Quellen und Senken in der exakten optischen Simulation", (Online-Zeitschrift der Deutschen Gesellschaft für angewandte Optik e. V.), ISSN: 1614-8436-urn:nbn:de:0287-2014-H004-1 115. Jahrestagung, 10.-14. Juni 2014, Karlsruhe, (2014)
6. X. Liu, K.-H. Brenner, "Einfluss der Kamera-Auflösung auf die spatiale Auflösung von Phase Retrieval", (Online-Zeitschrift der Deutschen Gesellschaft für angewandte Optik e. V.), ISSN: 1614-8436-urn:nbn:de:0287-2014-A012-3, 115. Jahrestagung, 10.-14. Juni 2014, Karlsruhe, (2014)

IMPRINT

Publisher: Prof. Dr. Karl-Heinz Brenner
Chair of Optoelectronics
Institute of Computer Engineering (ZITI)
Universität Heidelberg
B6, 23-29, Bauteil C
68131 Mannheim
GERMANY

 +49 (0) 621 181 2700
 +49 (0) 621 181 2695
 <http://oe.ziti.uni-heidelberg.de>

Layout: K.-H. Brenner, S. Volk

Type of publication: Online

Publication date: 2016

For quotation of any of these contributions, please use:

Reference: Annual Report 2014
Chair of Optoelectronics,
Universität Heidelberg
ISSN 2197 - 4462